

# Robust GNSS Navigation in Urban Environments by Bounding NLOS Bias of GNSS Pseudoranges Using a 3D City Model

N. Kbayer, M. Sahnoudi, E. Chaumette  
ISAE-SUPAERO, Université de Toulouse, France,  
Mail: {nabil.kbayer, mohamed.sahnoudi, eric.chaumette}@isae.fr

## BIOGRAPHIES

**Nabil Kbayer** is a PhD student at the French Institute of Aeronautics and Space (ISAE-SUPAERO), University of Toulouse, France. He received his engineer degree in signal processing from the French Institute of Aeronautics and Space (ISAE-ENSICA). His research interests include signal processing for positioning in challenging environments, multipath and NLOS mitigation and constructive use for cognitive navigation.

**Mohamed Sahnoudi** received a PhD in signal processing and communications systems from Paris-Sud Orsay University, France, in collaboration with Telecom Paris in 2004. From 2005 to 2007, he was a post-doctoral researcher fellow on GPS Signal Processing and Navigation at Villanova University, PA, USA. In august 2007, he joined the ETS school of engineering at Montreal, Canada, to lead the research team of precise positioning (RTK and PPP). In 2009 he became an Associate Professor at the French Institute of Aeronautics and Space (ISAE-SUPAERO), University of Toulouse, France. Currently his research interests focus on all aspects of signal processing for navigation and positioning in harsh environment, weak GNSS signals acquisition and tracking, multi-frequency and multi-GNSS receivers, multipath mitigation and constructive use and multi-sensor fusion for robust navigation.

**Eric Chaumette** was born in 1965 at Chartres (France). He studied Electronics and Signal Processing both at ENAC (Toulouse, France), where he obtained a diploma of engineer in 1989, and at Toulouse University where he obtained a M.Sc. degree in Signal Processing in 1989. From 1990 to 2007, he was with Thales in the radar studies departments and received a PhD degree in 2004 at laboratory SATIE, CNRS, *Ecole Normale Supérieure de Cachan*, France. From 2007 to 2013, he was with the Electromagnetic and Radar Division of the French Aerospace Lab (ONERA), Palaiseau, France, as a research engineer. He is now with the Department of Electronics, Optronics and Signal of the French Institute of Aeronautics and Space (ISAE-SUPAERO). Main domains of interest are related to radar scene modelling, detection and estimation theory and navigation.

## ABSTRACT

The well-known conventional Weighted Least Squares (WLS) and extended Kalman filter (EKF) are the standard estimation methods for positioning with GNSS measurements. However, these estimators are not optimal when the GNSS measurements become contaminated by non-Gaussian errors including multipath (MP) and non-line-of-sight (NLOS) biases. In this paper, we use additional information of the geometric environment provided by a 3D model to build-up a robust solution against biases which may be summed up from MP and NLOS signals in urban environments. We first use a 3D city model to predict lower and upper bounds of these biases. Then, we integrate this information in the position estimation problem. We investigated in two ways of making use of this additional information: the first one is to consider these biases as additive noise and exploiting the bounds to end up with a constrained state estimation by WLS or Kalman filter. The second way is to investigate in the maximum likelihood estimation of both the MP-NLOS bias and the state ending up with a less accurate but acceptable solution. Test results using real GPS signal in Toulouse show that these estimators capable of improving the positioning accuracy compared to the conventional WLS if the NLOS bounds are well-chosen.

## NOTATION

The notational convention adopted is as follows: italic indicates a scalar quantity, as in  $a$ ; lower case boldface indicates a column vector quantity, as in  $\mathbf{a}$ ; upper case boldface indicates a matrix quantity, as in  $\mathbf{A}$ ; The  $n$ -th row and the  $m$ -th column element of the matrix  $\mathbf{A}$  will be denoted by  $a_{n,m}$  or  $(\mathbf{A})_{n,m}$ . The  $n$ -th coordinate of the column vector  $\mathbf{a}$  will be denoted by  $a_n$  or  $(\mathbf{a})_n$ . The matrix/vector transpose conjugate is indicated by a superscript  $\text{T}$  as in  $\mathbf{A}^{\text{T}}$ . The inverse of a matrix is indicated by a superscript  $^{-1}$  as in  $\mathbf{A}^{-1}$ .  $[\mathbf{A}, \mathbf{B}]$  denotes the matrix resulting from the horizontal concatenation of matrix  $\mathbf{A}$  and  $\mathbf{B}$ .  $(\mathbf{a}^{\text{T}}, \mathbf{b}^{\text{T}})$  denotes the row vector resulting from the horizontal concatenation of row vectors  $\mathbf{a}^{\text{T}}$  and  $\mathbf{b}^{\text{T}}$ .  $\mathbf{I}_m$  is the identity matrix of order  $m$ .  $S^{\perp}$  denotes the orthogonal

complement of the subspace  $\mathcal{S}$ .  $\mathbf{1}$  denotes the column vector containing only the value 1.  $\langle \mathbf{a} | \mathbf{b} \rangle$  denotes the scalar product of vector  $\mathbf{a}$  and  $\mathbf{b}$ ,  $\|\mathbf{a}\|$  denotes the norm of the vector  $\mathbf{a}$ . If  $\boldsymbol{\theta} = (\theta_1, \theta_2, \dots, \theta_p)^T$ , then  $\frac{\partial}{\partial \boldsymbol{\theta}} = \left( \frac{\partial}{\partial \theta_1}, \frac{\partial}{\partial \theta_2}, \dots, \frac{\partial}{\partial \theta_p} \right)^T$ .

## INTRODUCTION

Global Navigation Satellite systems (GNSS) have emerged as powerful technology for providing the geolocation solution essential for a wide range of applications and services. The last two decades have seen a growing trend towards the use of GNSS for positioning in urban environments, because of the steep increase of applications relying on geolocation in these environments. However, the reliability of these systems can be adversely affected under certain conditions in this kind of harsh environments. The positioning quality cannot be ensured in general when traversing a harsh environment (urban, forested or mountainous areas or inside buildings) even for the majority of comfort applications requiring few meters of accuracy. Indeed, these environments present significant challenges for satellites positioning which explains the gap between user expectations and requirements from one side and the existing technologies from other side. One of the greatest reasons of that GNSS performance in harsh urban setting is the high density of tall buildings and objects blocking the direct line-of-sight (LOS) signal from many satellites, which may reduce the visibility of available satellites in view. Often, the received signals have poor geometry and therefore degrade the position accuracy.

In addition, the density of various obstacles surrounding the GNSS receiver leads to receiving reflected and diffracted signals from buildings and other objects. This situation produces a distortion of the pseudo-range (PR) measurements and consequently biases the position calculation. There are two types of signals received in indirect paths: Multipath (MP) signal if the signal is received through both direct line of sight (LOS) and indirect path and Non-Line-Of-Sight (NLOS) signal if the signal is received only through reflections. Even though both the NLOS reception and multipath interference are often grouped together as “multipath”, they are actually separate phenomena that cause very different ranging errors [2]. Therefore, it is important to treat these two phenomena separately. To date, several studies have attempted to deal with the multipath problem through receiver-based techniques such as narrow-correlators [3, 4]. Whilst mature research works has been carried out on MP mitigation in presence of LOS, there are still very little scientific investigations to solve the NLOS difficult problem. In this paper, we introduce a new robust GNSS solution that use the 3D model of the environment to bound the NLOS bias and then mitigate its effect in the state estimation. This paper is divided into four main sections. In the first section, we propose a review of

studies on using 3D model to mitigate the NLOS phenomenon. Our contributions to bound the NLOS bias using the 3D model and then mitigate it in the state estimate will be detailed in section 2. In section 3, we show the results of comparison between our methods and other existing works using real GPS data collected in Toulouse (South-West of France). Performances are compared with an iterative Least Square [13]. Finally, some conclusions are summarized in the fourth section.

## EXISTING METHODS

One of the current main challenges in the use of GNSS for positioning in urban environments is the MP and NLOS bias present in the PR measurements. These biases induce biased position estimation with several meters of PR errors in some harsh environments [5]. In order to improve the performance of satellite navigation in these environments, many of existing techniques aim to model these degradations and mitigate their effects at the level of signal processing, measurements or position domain [6].

Since the conventional least squares method is not robust to bias errors [7], some studies have focused on making the estimation more robust to these outliers by minimizing other residual functional instead of the sum of squares of residuals used in the least squares solution such as the M-estimation techniques [6]-[12] and the Robust Extended Kalman Filtering [9, 11, 13, 14]. Although these estimators enhance the positioning performance and mitigate the effects of outliers present in measurements, a high number of biased measurements compared to reliable measurements lead to large positioning errors. This fact limits the use of robust methods without additional information in urban and deep urban environments when the majority of the available signals are contaminated with bias errors. A standard approach for dealing with this problem consists of enhancing the positioning robustness in the measurement domain by detecting and rejecting bad observables using RAIM methods or statistical tests [15, 16]. However RAIM methods assume the availability of at least five reliable measurements and at most one faulty pseudorange. To address the problem of identifying the contaminated measurements among the healthy measurements, [2] gives a survey on distinguishing NLOS measurements from LOS measurements. Some of the proposed methods investigate the use of an additional hardware allowing the NLOS-LOS signal distinction. Without using additional hardware, [2] proposes others criteria of distinction such as elevation angle selection, C/N0 selection and consistency checking [17]. Once NLOS measurements are identified, they can be either discarded [18], weighted [19] or used in a way which improves performances [20, 21, 22].

In urban and deep urban canyons characterized by reduced visibility and a lack of measurements, discarding all the faulty measurements will lead to not having a PVT solution since we need at least four measurements for the position estimation. So, recent studies have focused on

using constructively these NLOS observables to improve the measurements model [20-22]. One way of doing this is to predict the NLOS bias via aiding information from a 3D city model and then correct it in the PR measurements. 3D models used jointly with a GNSS simulator characterize on-the-fly the measurements errors in urban environments. With an initial position input, these models simulate the GNSS propagation in representative type of environments (e.g. open sky, urban and deep urban) and provide the user with several types of information such as the number and the characteristics of reflections, additional PR biases... The quality and reliability of the simulated signals and errors depend on how much close is the a priori input position to the actual position to be estimated. Refs [21] and [22] have used the 3D model to predict PR errors and use it constructively on the estimation step. To manage the problem of the vicinity between the input point in the 3D model and the unknown position to be estimated, some studies opt to use a grid of input points in the zone of interest. The estimation of the position is then provided by comparison between the observations present in the receiver level and one of the information provided by the 3D model such as the sky visibility [1], the delay information [23], the PR measurements [24, 25] and the position consistency [2]. Other approaches combine a simplified 3D model of the environment with a probabilistic method to enhance performances [26, 27].

The main challenge of using 3D models in the positioning problem is the choice of the input position and the reliability of the 3D model itself which is only a deterministic approximation of the reality. An input point not sufficiently close to the unknown position to be estimated may induce large positioning errors. Besides, although the 3D simulator are becoming more and more reliable, they contain a certain level of inaccuracy due to the impossibility of modeling the real-time moving objects in the receiver environment (cars, pedestrians, tracks,...) and some immovable but variable objects such as trees with different texture from Spring to Autumn. In addition, it is obvious that the predicted bias and errors from the 3D propagation model cannot be instantaneous and accurate. Therefore, we propose in this paper an original solution to handle this inaccuracy and this chicken and eggs problem between the input position choice and the fix to compute. Instead of using the exact value of the output bias provided by the 3D model, as it was classically done in previous studies, we will just use upper and lower bounds of these biases. We seek to study the problem of positioning with NLOS GNSS pseudoranges (PR) in urban canyons by using a 3D city model to predict the most appropriate bounds of the measurement bias. The idea is to predict lower and upper bounds of the each PR bias and integrate this information as additional inequality constraints in the position estimation problem. The resulting problem is more realistic in reduced satellites visibility scenarios than trying the instantaneous values. First, we define a grid of position candidates as input to the 3D model simulator SPRING provided by the French space agency CNES [28]

to obtain PR NLOS bias values for each satellite in visibility. We select only the maximum and minimum values of the bias for each satellite to define an admissible range of the measurements NLOS bias. We use these bounds to formalize the position estimation as an inequality constrained problem as it will be detailed in the next section. The final navigation solution is obtained via an iterative least-square solution with improved integrity and robustness as it will be shown in the results and analysis section.

## ROBUST GNSS NAVIGATION

The following nonlinear measurement equation formulates the satellite positioning problem at each time step:

$$\mathbf{r} = \mathbf{h}(\mathbf{x}) + \mathbf{1}b_c + \mathbf{b}_{MP-NLOS} + \mathbf{v} \quad (1)$$

where:  $\mathbf{x}$  is the state vector containing the values of the three coordinates of the user position to be estimated [M, 1],  $\mathbf{r}$  is the PR measurements vector [N,1] with  $N > M$ .  $\mathbf{h}(\mathbf{x})$  is the true distance between the satellite position and the receiver position,  $b_c$  is the clock bias which is common between all the satellites,  $\mathbf{b}_{MP-NLOS}$  is the measurement bias included in the measured pseudoranges and which is caused basically by MP and NLOS signals in urban environments [N, 1],  $\mathbf{v}$  is the measurement noise supposed to be a zero-mean Gaussian white noise characterized by a covariance matrix  $\mathbf{R}$ .

Let reword this problem by gathering the two bias errors  $\mathbf{b} = \mathbf{1}b_c + \mathbf{b}_{MP-NLOS}$  providing the following measurements model:

$$\mathbf{r} = \mathbf{h}(\mathbf{x}) + \mathbf{b} + \mathbf{v} .$$

We seek to estimate  $\mathbf{x}$  by the conditional maximum likelihood estimator which minimizes the observation probability density function (pdf) of the conditional Gaussian observation model [29]:

$$\hat{\mathbf{x}} = \arg \min_{\mathbf{x}} \{J(\mathbf{r}|\mathbf{x}, \mathbf{b})\} = \arg \left\{ \frac{\partial J(\mathbf{r}|\mathbf{x}, \mathbf{b})}{\partial \mathbf{x}} = 0 \right\} , \quad (2)$$

where  $J(\mathbf{r}|\mathbf{x}, \mathbf{b})$  is the cost function or the likelihood function to be minimized to estimate both  $\mathbf{x}$  and  $\mathbf{b}$ . This is a batch estimation method but the proposed scheme could be applied similarly to iterative estimation methods like the iterative WLS and Kalman filter.

The above cost function can be written as:

$$\begin{aligned} J(\mathbf{r}|\mathbf{x}, \mathbf{b}) &= \|\mathbf{r} - \mathbf{h}(\mathbf{x}) - \mathbf{b}\|_{\mathbf{R}^{-1}}^2 \\ &= (\mathbf{r} - \mathbf{h}(\mathbf{x}) - \mathbf{b})^T \mathbf{R}^{-1} (\mathbf{r} - \mathbf{h}(\mathbf{x}) - \mathbf{b}) \end{aligned} \quad (3)$$

Since the function  $\mathbf{h}(\mathbf{x})$  is nonlinear, this problem cannot be resolved analytically in general. To overcome this limitation, we can linearize this problem about a known reference point  $\mathbf{x}_0$ . The first order of Taylor expansion of the function  $\mathbf{h}(\mathbf{x})$  is equal to:

$$\begin{aligned}\mathbf{h}(\mathbf{x}) &\approx \mathbf{h}(\mathbf{x}_0) + \frac{\partial \mathbf{h}(\mathbf{x}_0)}{\partial \mathbf{x}} (\mathbf{x} - \mathbf{x}_0) \\ &= \mathbf{h}(\mathbf{x}_0) + \mathbf{H}_0 (\mathbf{x} - \mathbf{x}_0)\end{aligned}\quad (4)$$

This reference point  $\mathbf{x}_0$  should be close enough to the true receiver position  $\mathbf{x}$ . Practically speaking, we define  $\mathbf{x}_0$  as the estimated receiver position at the previous time step. If we define a linearized PR measurement vector  $\mathbf{y}$  equal to  $\mathbf{y} = \mathbf{r} - (\mathbf{h}(\mathbf{x}_0) - \mathbf{H}_0 \mathbf{x}_0)$  then the problem (1) can be formulated by the following linear measurement equation:

$$\mathbf{y} = \mathbf{H}_0 \mathbf{x} + \mathbf{1} b_c + \mathbf{b}_{MP-NLOS} + \mathbf{v} \quad (5)$$

It is important to note that the new position to be estimated is a position related to the reference point  $\mathbf{x}_0$  which may be chosen as the previous position estimation. Since the clock bias is the same for all the satellites then this problem can be restated as:

$$\mathbf{y} = \mathbf{A}_0 \mathbf{s} + \mathbf{b}_{MP-NLOS} + \mathbf{v} \quad (6)$$

where  $\mathbf{A}_0 = [\mathbf{H}_0 \ \mathbf{1}]$  and  $\mathbf{s}^T = (\mathbf{x}^T, b_c)$ . Then, the cost function used in the maximum likelihood estimator to estimate  $\mathbf{s}$  will be equal to:

$$\begin{aligned}J(\mathbf{r}|\mathbf{s}, \mathbf{b}) &\approx \|\mathbf{y} - \mathbf{A}_0 \mathbf{s} - \mathbf{b}_{MP-NLOS}\|_{\mathbf{R}^{-1}}^2 \\ J(\mathbf{r}|\mathbf{s}, \mathbf{b}) &\approx (\mathbf{y} - \mathbf{A}_0 \mathbf{s} - \mathbf{b}_{MP-NLOS})^T \mathbf{R}^{-1} (\mathbf{y} - \mathbf{A}_0 \mathbf{s} - \mathbf{b}_{MP-NLOS})\end{aligned}\quad (7)$$

Without having any information on the MP and NLOS measurement bias, the estimate of state vector  $\mathbf{s}$  will be biased. To compensate for the effect of MP/NLOS, we need some geometric information about the propagation paths of received signals. Therefore, we propose to use a 3D city model combined with a GNSS simulator to obtain a feasible range set of the MP-NLOS bias error. The propagation calculation uses ray-tracing methods. We assume that at every time step the measurement bias  $\mathbf{b}_{MP-NLOS}$  is bounded, meaning that:

$$\forall n = 1, 2, \dots, N, \quad (\mathbf{l})_n \leq (\mathbf{b}_{MP-NLOS})_n \leq (\mathbf{u})_n \quad (8)$$

where  $\mathbf{l} = [l_1, l_2, \dots, l_N]^T$  is the lower bound of the bias and  $\mathbf{u} = [u_1, u_2, \dots, u_N]^T$  is the upper bound of the bias.

The computation of these two bounds at every time step using a 3D city model will be detailed in the third section. We propose two solutions to exploit this additional information on the MP-NLOS bias. In the first part, we will use it directly in the position estimation problem to end up with a constrained least squares solution. In the second part, we will reformulate the problem and start by

estimating the additional bias and then exploit this estimation to correct the estimation of the state vector.

### Constrained Least Squares

Substituting the linear equation (6) on the NLOS bounding inequalities (8), we will obtain:

$$\forall n = 1, 2, \dots, N, \quad (\mathbf{l})_n \leq (\mathbf{y} - \mathbf{A}_0 \mathbf{s} - \mathbf{v})_n = (\mathbf{b}_{MP-NLOS})_n \leq (\mathbf{u})_n \quad (9)$$

This leads to:

$$\forall n = 1, 2, \dots, N, \quad (\mathbf{y})_n - (\mathbf{u})_n - (\mathbf{v})_n \leq (\mathbf{A}_0 \mathbf{s})_n \leq (\mathbf{y})_n - (\mathbf{l})_n - (\mathbf{v})_n \quad (10)$$

When the measurement noise is a zero-mean white Gaussian noise,  $(\mathbf{v})_n$  lies between  $-3\sigma_n$  and  $3\sigma_n$  with a probability of 99.73% where  $\sigma_n$  is the measurement noise variance for the measurement from the  $n^{\text{th}}$  satellite. This assumption allows us to obtain final bounds of  $(\mathbf{A}_0 \mathbf{s})$ :

$$\mathbf{c}_{\text{inf}} \leq \mathbf{A}_0 \mathbf{s} \leq \mathbf{c}_{\text{sup}} \quad (11)$$

where  $\mathbf{c}_{\text{inf}} = [y_1 - u_1 - 3\sigma_1, \dots, y_N - u_N - 3\sigma_N]$  is the lower bound and  $\mathbf{c}_{\text{sup}} = [y_1 - l_1 + 3\sigma_1, \dots, y_N - l_N + 3\sigma_N]$  is the upper bound.

In this method, we consider the bias as a noise component which will not be estimated by the maximum likelihood estimator. If the MP-NLOS bias will be removed from the expression of the cost function in (7), then it must be taken into account in the covariance matrix noise to improve the estimation of the state vectors  $\mathbf{s}$ . This means that the MP-NLOS bias will be considered –for now at this step– as a measurement noise and then the total measurement noise will be equal to:

$$\mathbf{n} = \mathbf{b}_{MP-NLOS} + \mathbf{v}$$

The bias  $\mathbf{b}_{MP-NLOS}$  lies between the NLOS bias lower bound  $\mathbf{l}$  and the NLOS bias upper bound  $\mathbf{u}$ . Since the values of the bias vector are unknown, we assume that every MP-NLOS bias value  $(\mathbf{b}_{MP-NLOS})_n$  has a Gaussian

distribution with a mean value equal to  $\frac{u_n + l_n}{2}$  and a

standard deviation equal to  $\frac{u_n - l_n}{6}$ . These mean and

standard deviation values are chosen to ensure that 99.73% of the bias values are within the interval  $[l_n, u_n]$  as shown in the following figure:

### MP-NLOS Bias Probability Density Function

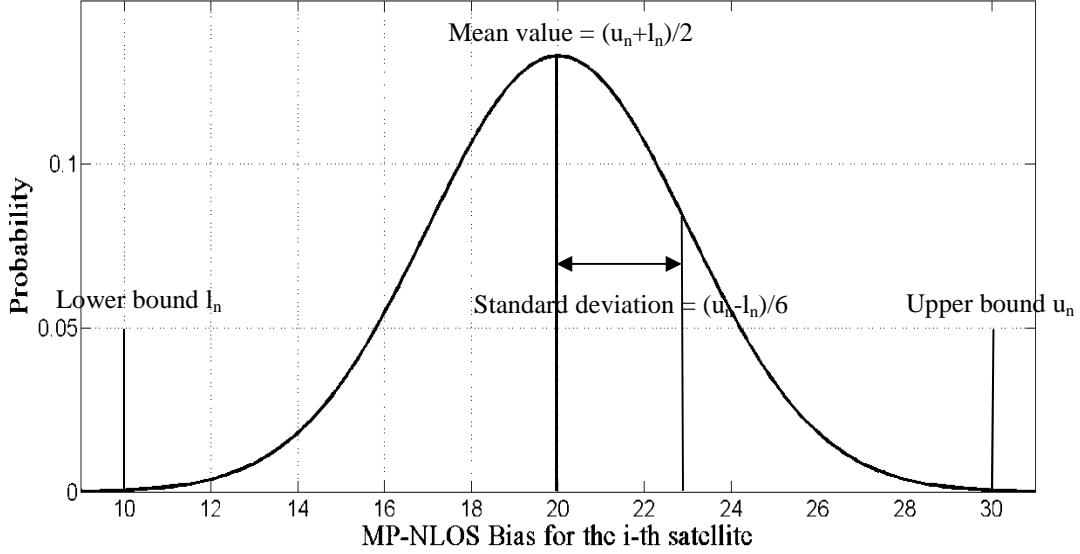


Figure 1: MP-NLOS bias Probability Density function

Since the MP-NLOS bias and the measurement noise are independent, the total noise  $\mathbf{n}$  will have a Gaussian distribution with a covariance matrix equal to:

$$\mathbf{R}_b = \mathbf{R} + \text{diag} \left\{ \left[ \frac{u_n - l_n}{6} \right]^2 \right\}_{n=1, \dots, N} \quad (12)$$

The mean value of the  $n^{\text{th}}$  coordinate of the total measurement noise  $(\mathbf{n})_n$  will be equal to  $\frac{u_n + l_n}{2}$  since the measurement noise  $\mathbf{v}$  is a zero-mean noise. This mean value must be subtracted from the PR measurement vector  $\mathbf{y}$  when estimating the state vector. Then, the corrected PR measurement will be noted  $\mathbf{y}_c$  such that:

$$\forall n = 1, 2, \dots, N, \quad (\mathbf{y}_c)_n = (\mathbf{y})_n - \frac{u_n + l_n}{2}.$$

It is worthy to note that some previous works subtract an estimated non-zero mean value from the pseudoranges before the PVT computation when detected as a non-zero jump in the mean values using a chi-square based statistical test of residuals. However, again a reliable residual test assumes that the PVT is accurate enough to be able to detect a jump in the measurements. In this work, we are interested to scenario where most or all the pseudoranges are contaminated by MP or NLOS errors.

Finally, the constrained least square solution of the problem (6) is:

$$\begin{cases} \hat{\mathbf{s}} = \underset{\mathbf{s}}{\text{argmin}} \|\mathbf{y}_c - \mathbf{A}_0 \mathbf{s}\|_{\mathbf{R}_b^{-1}}^2 = \underset{\mathbf{s}}{\text{argmin}} (\mathbf{y}_c - \mathbf{A}_0 \mathbf{s})^T \mathbf{R}_b^{-1} (\mathbf{y}_c - \mathbf{A}_0 \mathbf{s}) \\ \text{subject to} \quad \mathbf{c}_{\text{inf}} \leq \mathbf{A}_0 \mathbf{s} \leq \mathbf{c}_{\text{sup}} \end{cases} \quad (13)$$

This problem is equivalent to the following constrained quadratic system:

$$\begin{cases} \hat{\mathbf{s}} = \underset{\mathbf{s}}{\text{argmin}} \mathbf{s}^T (\mathbf{A}_0^T \mathbf{R}_b^{-1} \mathbf{A}_0) \mathbf{s} - 2(\mathbf{y}_c^T \mathbf{R}_b^{-1} \mathbf{A}_0) \mathbf{s} \\ \text{subject to} \quad \begin{bmatrix} \mathbf{A}_0 \\ -\mathbf{A}_0 \end{bmatrix} \mathbf{s} \leq \begin{bmatrix} \mathbf{c}_{\text{sup}} \\ -\mathbf{c}_{\text{inf}} \end{bmatrix} \end{cases} \quad (14)$$

This quadratic problem can be resolved using the Matlab routine *quadprog*. This estimator will be referred as the Constrained Iterative Least Squares (CILS).

### Maximum likelihood estimation of the State and Bias vectors

Let us define the following scalar product related to the matrix  $\mathbf{R}$ :

$$\forall \mathbf{a}, \mathbf{c} \in \mathfrak{R}^N, \quad \langle \mathbf{a} | \mathbf{c} \rangle_{\mathbf{R}^{-1}} = \mathbf{a}^T \mathbf{R}^{-1} \mathbf{c} \quad (15)$$

The corresponding norm is then:

$$\forall \mathbf{a} \in \mathfrak{R}^N, \quad \|\mathbf{a}\|_{\mathbf{R}^{-1}}^2 = \mathbf{a}^T \mathbf{R}^{-1} \mathbf{a} \quad (16)$$

We can define the orthogonal projection on  $\mathbf{A}_0$  with regard to this scalar product:

$$\forall \mathbf{a} \in \mathfrak{R}^N, \quad \Pi_{\mathbf{R}^{-1}}^{\mathbf{A}_0} \mathbf{a} = \mathbf{A}_0 (\mathbf{A}_0^T \mathbf{R}^{-1} \mathbf{A}_0)^{-1} \mathbf{A}_0^T \mathbf{R}^{-1} \mathbf{a} \quad (17)$$

Let  $\mathbf{A}_0^\perp$  be the vector subspace orthogonal to  $\mathbf{A}_0$  with regard to the scalar product (15). The orthogonal projection on this subspace is equal to:

$$\forall \mathbf{a} \in \mathfrak{R}^N, \quad \Pi_{\mathbf{R}^{-1}}^{\mathbf{A}_0^\perp} \mathbf{a} = \mathbf{a} - \Pi_{\mathbf{R}^{-1}}^{\mathbf{A}_0} \mathbf{a} = (\mathbf{I}_N - \Pi_{\mathbf{R}^{-1}}^{\mathbf{A}_0}) \mathbf{a} \quad (18)$$

Let us express now the cost function in (7):

$$\begin{aligned}
J(\mathbf{y}|\mathbf{s}, \mathbf{b}_{MP-NLOS}) &= \left\| \mathbf{y} - \mathbf{A}_0 \mathbf{s} - \mathbf{b}_{MP-NLOS} \right\|_{\mathbf{R}^{-1}}^2 \\
&= \left\| (\Pi_{\mathbf{R}^{-1}}^{\mathbf{A}_0^\perp} + \Pi_{\mathbf{R}^{-1}}^{\mathbf{A}_0}) (\mathbf{y} - \mathbf{A}_0 \mathbf{s} - \mathbf{b}_{MP-NLOS}) \right\|_{\mathbf{R}^{-1}}^2 \\
&= \left\| (\Pi_{\mathbf{R}^{-1}}^{\mathbf{A}_0}) (\mathbf{y} - \mathbf{A}_0 \mathbf{s} - \mathbf{b}_{MP-NLOS}) \right\|_{\mathbf{R}^{-1}}^2 \\
&\quad + \left\| (\Pi_{\mathbf{R}^{-1}}^{\mathbf{A}_0^\perp}) (\mathbf{y} - \mathbf{A}_0 \mathbf{s} - \mathbf{b}_{MP-NLOS}) \right\|_{\mathbf{R}^{-1}}^2 \\
&= \left\| (\Pi_{\mathbf{R}^{-1}}^{\mathbf{A}_0}) (\mathbf{y} - \mathbf{b}_{MP-NLOS}) - \mathbf{A}_0 \mathbf{s} \right\|_{\mathbf{R}^{-1}}^2 \\
&\quad + \left\| (\Pi_{\mathbf{R}^{-1}}^{\mathbf{A}_0^\perp}) (\mathbf{y} - \mathbf{b}_{MP-NLOS}) \right\|_{\mathbf{R}^{-1}}^2
\end{aligned} \tag{19}$$

The state estimate is then equal to:

$$\begin{aligned}
\hat{\mathbf{s}} &= \underset{\mathbf{s}}{\operatorname{argmin}} \left\{ J(\mathbf{y}|\mathbf{s}, \mathbf{b}_{MP-NLOS}) \right\} \\
&= \underset{\mathbf{s}}{\operatorname{argmin}} \left\{ \left\| (\Pi_{\mathbf{R}^{-1}}^{\mathbf{A}_0}) (\mathbf{y} - \mathbf{b}_{MP-NLOS}) - \mathbf{A}_0 \mathbf{s} \right\|_{\mathbf{R}^{-1}}^2 \right. \\
&\quad \left. + \left\| (\Pi_{\mathbf{R}^{-1}}^{\mathbf{A}_0^\perp}) (\mathbf{y} - \mathbf{b}_{MP-NLOS}) \right\|_{\mathbf{R}^{-1}}^2 \right\} \\
&= \underset{\mathbf{s}}{\operatorname{argmin}} \left\{ \left\| (\Pi_{\mathbf{R}^{-1}}^{\mathbf{A}_0}) (\mathbf{y} - \mathbf{b}_{MP-NLOS}) - \mathbf{A}_0 \mathbf{s} \right\|_{\mathbf{R}^{-1}}^2 \right\} \\
&= \underset{\mathbf{s}}{\operatorname{argmin}} \left\{ \left\| \mathbf{A}_0 (\mathbf{A}_0^T \mathbf{R}^{-1} \mathbf{A}_0)^{-1} \mathbf{A}_0^T \mathbf{R}^{-1} (\mathbf{y} - \mathbf{b}_{MP-NLOS}) - \mathbf{A}_0 \mathbf{s} \right\|_{\mathbf{R}^{-1}}^2 \right\} \\
&= \underset{\mathbf{s}}{\operatorname{argmin}} \left\{ \left\| \mathbf{A}_0 \left[ (\mathbf{A}_0^T \mathbf{R}^{-1} \mathbf{A}_0)^{-1} \mathbf{A}_0^T \mathbf{R}^{-1} (\mathbf{y} - \mathbf{b}_{MP-NLOS}) - \mathbf{s} \right] \right\|_{\mathbf{R}^{-1}}^2 \right\} \\
&= (\mathbf{A}_0^T \mathbf{R}^{-1} \mathbf{A}_0)^{-1} \mathbf{A}_0^T \mathbf{R}^{-1} (\mathbf{y} - \mathbf{b}_{MP-NLOS})
\end{aligned} \tag{20}$$

The maximum likelihood state estimation is equal to the least squares solution by considering the PR measurement corrected by the MP-NLOS bias. This state estimation can be seen as a sum of a bias free-estimate computed as if no MP and NLOS bias were present and a bias-correction term. Without knowing the MP-NLOS bias value, the estimation of the state vector will be inaccurate. Then, we propose to estimate this bias to use in the correction of the state estimation using equation (20).

The MP-NLOS bias  $\mathbf{b}_{MP-NLOS}$  can be estimated by minimizing the cost function regard to  $\mathbf{b}_{MP-NLOS}$ :

$$\begin{aligned}
\hat{\mathbf{b}}_{MP-NLOS} &= \underset{\mathbf{b}_{MP-NLOS}}{\operatorname{argmin}} \left\{ J(\mathbf{y}|\hat{\mathbf{s}}, \mathbf{b}_{MP-NLOS}) \right\} \\
&= \underset{\mathbf{b}_{MP-NLOS}}{\operatorname{argmin}} \left\{ \left\| (\Pi_{\mathbf{R}^{-1}}^{\mathbf{A}_0}) (\mathbf{y} - \mathbf{b}_{MP-NLOS}) - \mathbf{A}_0 \hat{\mathbf{s}} \right\|_{\mathbf{R}^{-1}}^2 \right. \\
&\quad \left. + \left\| (\Pi_{\mathbf{R}^{-1}}^{\mathbf{A}_0^\perp}) (\mathbf{y} - \mathbf{b}_{MP-NLOS}) \right\|_{\mathbf{R}^{-1}}^2 \right\} \\
&= \underset{\mathbf{b}_{MP-NLOS}}{\operatorname{argmin}} \left\{ \left\| (\Pi_{\mathbf{R}^{-1}}^{\mathbf{A}_0^\perp}) (\mathbf{y} - \mathbf{b}_{MP-NLOS}) \right\|_{\mathbf{R}^{-1}}^2 \right\} \\
&= \underset{\mathbf{b}_{MP-NLOS}}{\operatorname{argmin}} \left\{ \left\| (\Pi_{\mathbf{R}^{-1}}^{\mathbf{A}_0^\perp}) \mathbf{y} - (\Pi_{\mathbf{R}^{-1}}^{\mathbf{A}_0^\perp}) \mathbf{b}_{MP-NLOS} \right\|_{\mathbf{R}^{-1}}^2 \right\}
\end{aligned} \tag{21}$$

Let us define  $\mathbf{y}_b = (\Pi_{\mathbf{R}^{-1}}^{\mathbf{A}_0^\perp}) \cdot \mathbf{y}$ . Then, we have:

$$\begin{aligned}
(\Pi_{\mathbf{R}^{-1}}^{\mathbf{A}_0^\perp}) \hat{\mathbf{b}}_{MP-NLOS} &= (\mathbf{I}_N - \Pi_{\mathbf{R}^{-1}}^{\mathbf{A}_0}) \hat{\mathbf{b}}_{MP-NLOS} \\
&= (\mathbf{I}_N - \mathbf{A}_0 (\mathbf{A}_0^T \mathbf{R}^{-1} \mathbf{A}_0)^{-1} \mathbf{A}_0^T \mathbf{R}^{-1}) \hat{\mathbf{b}}_{MP-NLOS} \\
&= \mathbf{A}_b \hat{\mathbf{b}}_{MP-NLOS}
\end{aligned}$$

The MP-NLOS bias estimate is then equal to:

$$\hat{\mathbf{b}}_{MP-NLOS} = \underset{\mathbf{b}_{MP-NLOS}}{\operatorname{argmin}} \left\{ \left\| \mathbf{y}_b - \mathbf{A}_b \mathbf{b}_{MP-NLOS} \right\|_{\mathbf{R}^{-1}}^2 \right\} \tag{22}$$

By using the same method of resolution as in (20), we get:

$$\hat{\mathbf{b}}_{MP-NLOS} = (\mathbf{A}_b^T \mathbf{R}^{-1} \mathbf{A}_b)^{-1} \mathbf{A}_b^T \mathbf{R}^{-1} \mathbf{y}_b \tag{23}$$

Noting that:

$$\begin{aligned}
\mathbf{b}_{MP-NLOS} &= (\Pi_{\mathbf{R}^{-1}}^{\mathbf{A}_0^\perp} + \Pi_{\mathbf{R}^{-1}}^{\mathbf{A}_0}) \mathbf{b}_{MP-NLOS} \\
&= \Pi_{\mathbf{R}^{-1}}^{\mathbf{A}_0^\perp} \mathbf{b}_{MP-NLOS} + \Pi_{\mathbf{R}^{-1}}^{\mathbf{A}_0} \mathbf{b}_{MP-NLOS} \\
&= \mathbf{b}_{MP-NLOS}^{\mathbf{A}_0^\perp} + \mathbf{b}_{MP-NLOS}^{\mathbf{A}_0}
\end{aligned}$$

we can conclude that what we have estimated is in fact the orthogonal projection of  $\mathbf{b}_{MP-NLOS}$  on the vector subspace  $\mathbf{A}_0^\perp$  since  $\mathbf{y}_b$  is the orthogonal projection of  $\mathbf{y}$  on this subspace then we have  $\hat{\mathbf{b}}_{MP-NLOS} = \mathbf{b}_{MP-NLOS}^{\mathbf{A}_0^\perp}$ . We can only estimate (N-M) components of the bias vector  $\mathbf{b}_{MP-NLOS}$  which is equals to the dimension of the subspace  $\mathbf{A}_0^\perp$  where M denotes the size of the state vector and N is the number of PR measurements. To correctly estimate the bias, we have to estimate the other component of the MP-NLOS bias  $\mathbf{b}_{MP-NLOS}^{\mathbf{A}_0}$ .

To overcome this problem, we propose to use the NLOS bounding information. The upper and lower bounds on each MP-NLOS bias component define a region B of the space  $\mathfrak{R}^N$  where the best estimate of the bias could be. Then, we seek to find a point  $\hat{\mathbf{b}}_{MP-NLOS}$  on this region B that have an orthogonal projection on the vector subspace  $\mathbf{A}_0^\perp$  verifying the equation (22). The final estimate of the bias would be:

$$\begin{cases} \hat{\mathbf{b}}_{MP-NLOS} = \hat{\mathbf{b}}_{MP-NLOS}^{\mathbf{A}_0^\perp} + \hat{\mathbf{b}}_{MP-NLOS}^{\mathbf{A}_0} \\ \text{with } \hat{\mathbf{b}}_{MP-NLOS}^{\mathbf{A}_0^\perp} = \underset{\mathbf{b}_{MP-NLOS}}{\operatorname{argmin}} \left\{ \left\| \mathbf{y}_b - \mathbf{A}_b \mathbf{b}_{MP-NLOS} \right\|_{\mathbf{R}^{-1}}^2 \right\} \\ \text{and } \hat{\mathbf{b}}_{MP-NLOS} \in \mathbf{B} \end{cases} \tag{24}$$

Authors of [30] estimate the bias in a similar way to our proposed method but the final estimate is not the same. In [30] the bias estimate is on the vector subspace  $\mathbf{A}_0^\perp$  and this estimate is not necessarily equals to the bias component on the subspace  $\mathbf{A}_0^\perp$ , because of the added box constraints B. Then, the bias estimate in [30] is not the maximum likelihood estimate of the MP-NLOS bias  $\mathbf{b}_{MP-NLOS}$  which means that this estimate will no longer be asymptotically (at high bias to noise ratio) efficient. But the additional information on the bias error which is the bounds allows

limiting this degradation. But in our method, we seek to estimate firstly the component of the bias in the vector subspace  $\mathbf{A}_0^\perp$  and then we look into the box constraints  $\mathbf{B}$  to find the vector that have a component in the subspace  $\mathbf{A}_0^\perp$  equals to the estimated one. If several points are found, then the final point will be the average of all these points. Since the problem (24) is difficult to solve, we have chosen to estimate the MP-NLOS bias as a solution of the constrained system composed of the minimization problem (22) and the box constraints  $\mathbf{B}$ .

Once the MP-NLOS bias is estimated, we use equation (20) to estimate the state vector by adding the bias-correction term to the bias-free term computed with the PR measurements as if no bias exists. Then, this estimation is called Iterative Least Squares with Bias Correction (ILSBC).

### NLOS bias bounding using 3D model

In this section, we will explain the strategy used to predict the most appropriate bounds of the measurement bias at each time step. The choice of the most suitable range set of the bias error is important for better estimation of the NLOS bias  $\mathbf{b}_k$  where  $k$  indicates the time step. Since these bounds are not known and highly dependent on the environment, we suggest in our work to use a 3D city model to predict lower and upper bounds of the each PR bias and integrate this information as additional inequality constraints in the position estimation problem as shown in the previous section.

We distinguish between two kinds of 3D models: ones providing pure geometrical information on the building and street sizes [1, 26] and others more informative providing also simulated GNSS signals at any input position and time [21, 22, 31]. In our study, we have used the software simulator SPRING provided by the French space agency CNES-Toulouse [28] to estimate the feasible range set of the bias errors. SPRING is a full software simulator that models the pseudo-range measurement and calculates the PVT solution considering the 3D environment of the receiver antenna. At each time step, the 3D model is applied in a set of inputs points that allows the calculation of the bias error on each received signal. In this work, we integrate the bound of this geometric information to improve the PVT solution. As the estimation of the NLOS bias bounds must be accurate enough, the inputs points used in the 3D model to obtain these bounds must be carefully chosen. To make this prediction of the bounds more accurate, we have used the following process to select the input points at each time step:

- The initial point is generated using a conventional GNSS solution (WLS or EKF): a search area around this point is defined as a square area centered on this solution and covering the area included in the available 3D city model. The size of this search area is defined according to the

environment and the integrity of the provided conventional GNSS solution.

- Elimination of indoor points from the defined search area because this method is applied to outdoor urban positioning. This step is achieved by a pre-processing of the search area in the 3D city model.

- Defining a number of random grid points in the search area that satisfy the same visibility condition. By visibility condition we mean that the received signals at each defined grid point has to be similar to the received signals by the receiver. A random grid points will give a better bounds prediction than a distributed grid points. The number of points used at each time step will be fixed depending on the computational cost and the size of the search area.

We obtain then a set of  $K$  points distributed randomly in the search area. For each of these points, the 3D city model will be applied to estimate the NLOS bias at this point for each received signal. Thus, for each point of the  $K$  grid points, we can define a NLOS bias vector:

$$\mathbf{b}_k = \begin{pmatrix} (\mathbf{b}_k)_1 \\ \cdot \\ \cdot \\ \cdot \\ (\mathbf{b}_k)_N \end{pmatrix} \quad \text{where } k=1, 2, \dots, K \text{ is the point index and}$$

$N$  is the number of received signals

Then the predicted bias bounds will be equal to:

$$\mathbf{l} = \begin{pmatrix} \min_k [(\mathbf{b}_k)_1] \\ \cdot \\ \cdot \\ \cdot \\ \min_k [(\mathbf{b}_k)_N] \end{pmatrix} \quad \text{and} \quad \mathbf{u} = \begin{pmatrix} \max_k [(\mathbf{b}_k)_1] \\ \cdot \\ \cdot \\ \cdot \\ \max_k [(\mathbf{b}_k)_N] \end{pmatrix} \quad \text{where } \mathbf{l} \text{ the lower}$$

bound vector and  $\mathbf{u}$  is the upper bound vector.

The inaccuracy of bias estimation using a 3D model simulator can be taken into account by adding a small variance, indicative of 3D modeling errors, to the lower and upper bounds prediction so that the final bounds prediction became:

$$\mathbf{l}_f = \mathbf{l} - (\sigma_i)_{i=1, \dots, N} \quad \text{and} \quad \mathbf{u}_f = \mathbf{u} + (\alpha_i)_{i=1, \dots, N}.$$

## RESULTS AND ANALYSIS

To assess the performance of the proposed positioning algorithms of GNSS, preliminary results are obtained from measurements collected in the ISAE-SUPAERO campus. The recorded GPS L1 C/A code PR measurements contain 3500 epochs. The data for the experiments were collected along the trajectory displayed in figure (2) of ISAE-SUPAERO campus. The recorded data corresponds to open sky conditions. In addition, we have eliminated the initial bias that exists in measurements. To do this, we have used the reference receiver positions and the

assumption that the highest elevation satellite corresponds to a line of sight (LOS) situation or to a weak MP-NLOS bias. The PR difference between the satellite with the highest elevation angle and other satellites allows us to have an approximate prediction of the initial bias present in measurements by neglecting measurements noise terms. In this section, we have manually introduced artificial biases and bounds prediction, but further results with 3D model bias prediction using SPRING [28] in downtown of Toulouse will be presented in next studies.

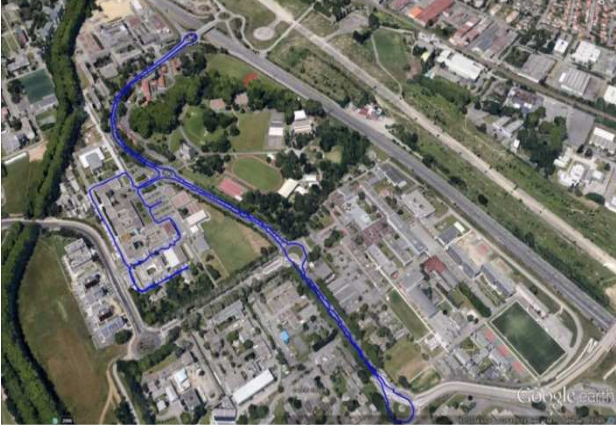


**Figure 2: Trajectory for data collection in ISAE-SUPAERO campus [32]**

We added artificial values of bias to some PR measurements to test the performances of our methods. First, we have considered only four signals among the eight received signals from the satellites in view during the measurement campaign. This scenario is more interesting to study because it corresponds to limited received signals as in urban canyons areas. We have added additional bias to these four signals. We have introduced biases between the epoch time 400 and the epoch time 2100. We have added a random bias between 0 meters and 40 meters to

the first PR measurement, a fixed bias of 60 meters to the second PR measurement, a random bias between 100 meters and 110 meters to the third PR measurement and a random bias between 20 meters and 30 meters to the fourth PR measurement. We have introduced the following upper and lower bounds between the epoch time 400 and the

epoch time 1800:  $\mathbf{l} = \begin{pmatrix} 0 \\ 55 \\ 95 \\ 18 \end{pmatrix}$  and  $\mathbf{u} = \begin{pmatrix} 41 \\ 63 \\ 114 \\ 32 \end{pmatrix}$ . Outside this

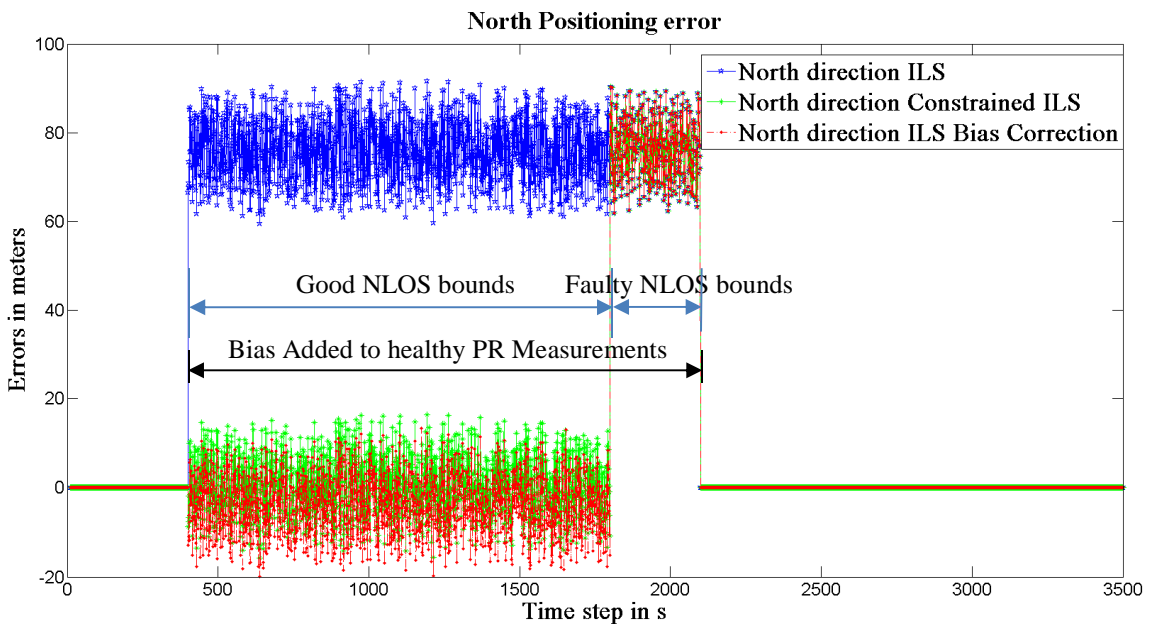
interval, we have considered the following upper and

lower bounds:  $\mathbf{l} = \begin{pmatrix} 0 \\ 0 \\ 0 \\ 0 \end{pmatrix}$  and  $\mathbf{u} = \begin{pmatrix} 0.75 \\ 0.75 \\ 0.75 \\ 0.75 \end{pmatrix}$ .

We have introduced faulty bounds between the epoch time 1800 and the epoch time 2100 to analyze the effect of bad bounding on the performances of the proposed methods. Finally, we used the UBLOX 4T receiver and a SPAN Novatel system including a DGPS receiver tightly integrated with an IMU-FSAS (from iMAR). We consider the trajectory provided by the Novatel receiver as the reference trajectory for comparison with our algorithms. We will compare our methods to the Iterative Least Square (ILS) [33]. The ILS argues that the state estimate at the epoch time  $k$  depends on the state estimate at the previous epoch time following this equation:

$$\mathbf{s}_k = (\mathbf{A}_0^T \mathbf{R}^{-1} \mathbf{A}_0)^{-1} \mathbf{A}_0^T \mathbf{R}^{-1} (\mathbf{y} - \mathbf{A}_0 \mathbf{s}_{k-1}) + \mathbf{s}_{k-1}$$

The following figures show the result of position estimation errors for the three methods: ILS, Constrained ILS and ILS with Bias correction. The results are shown in the north and east directions.





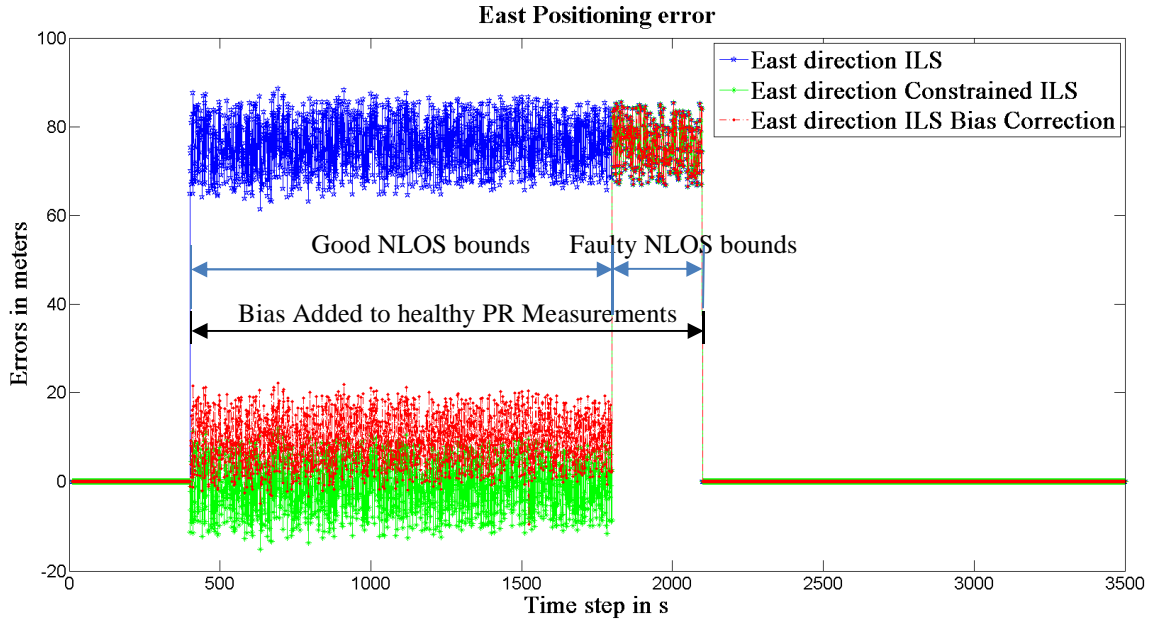


**Figure 3: North Positioning error (top) and East Positioning error (bottom)**

These figures show that the proposed two methods give the same performances as the ILS when there is no MP-NLOS bias in the PR measurements. They give less positioning errors when there are errors in the measurements as shown in the north and east positioning error in the time interval [400, 1800]. However the time interval [1800, 2100] shows that bad NLOS bounds can lead to bad performances for both methods. But, in general, the proposed methods handle well the problem of

the bias added in the PR measurements. To highlight this result, we compute the median, the 5<sup>th</sup> percentile, the 95<sup>th</sup> percentile and the maximum value of the positioning error in each ENU direction and for all estimators. In the following table, we have introduced the good NLOS bounds for the time interval [1800, 2100]:

**Table 1 : Performance evaluation of the three estimators**

	North Direction				East Direction			
	Median Positioning error [m]	5 <sup>th</sup> percentile [m]	95 <sup>th</sup> percentile [m]	Maximum Positioning error [m]	median Positioning error [m]	5 <sup>th</sup> percentile [m]	95 <sup>th</sup> percentile [m]	Maximum Positioning error [m]
Iterative Least Squares (ILS)	71.47e-06	43.25e-06	85.20	91.10	8.63e-06	-13.60e-08	83.46	89.33
Constrained Iterative Least Squares (CILS)	45.09e-06	-8.91	10.09	15.87	-2.56e-09	-8.87	6.42	14.51
Iterative Least Squares with Bias Correction (ILSBC)	44.98e-06	-13.14	5.79	19.72	2.67e-06	-22.07e-08	17.18	23.17
	Up direction							
	Median Positioning error [m]	5 <sup>th</sup> percentile [m]	95 <sup>th</sup> percentile [m]	Maximum Positioning error [m]				
Iterative Least Squares (ILS)	-223.36e-06		-87.18		62.09e-06	111.44		
Constrained Iterative Least Squares (CILS)	40.78e-06		-25.59		27.32	49.48		
Iterative Least Squares with Bias Correction (LSBC)	41.63e-06		-16.73		36.05	57.97		

It can be seen that the CILS and the ILSBC improve the positioning accuracy by being robust to the bias introduced into the PR measurements. These estimators give better performances than the conventional Iterative Least Squares. Despite this performance-improvement, the use of these estimators lead to erroneous results when the bias bounding is faulty which means that these methods are very depending on good lower and upper bounds prediction. We can notice also that the size of the NLOS bias constraints have few influence on the performance of the solution estimation, even though more narrow and accurate bounds lead to better performances especially for the CILS estimator, but the most critical condition is that the true bias value must be within the lower and upper bounds used in the estimation.

## CONCLUSIONS AND FUTUR WORKS

The purpose of this paper is to study the problem of positioning with NLOS GNSS pseudoranges in urban canyons by using a 3D city model to find the most appropriate bounds of the measurement bias and introducing these bounds in the state estimation to render the conventional least squares more robust to both MP and NLOS phenomena. In this work, we use firstly the 3D model simulator SPRING provided by the French Space Agency CNES to obtain an admissible range of the NLOS bias for each satellite in visibility. Then, we integrate this additional information in the state estimation ending with a constrained problem if we consider the bias as an additive noise or a maximum likelihood estimation of the state and the bias if not. Based on the obtained results, the two proposed methods seem to outperform the conventional Iterative Least Squares when a bias measurement occurs.

The current results show that the two proposed estimators are very sensitive to the quality of the predicted bounds. Faulty lower and upper bounds may lead to erroneous results as shown in the previous section. The steady improvement of the reliability of 3D models simulators may limit the damage of bad feasible bounds estimation. But generally speaking, these estimators provide an autonomous robust navigation solution for MP/NLOS mitigation purposes in urban environments even without enough redundancy of satellites in visibility.

The performance-improvement shown in the results section encourages us to more investigate in our methods and to validate them in deep urban environments. Besides, we will investigate on more accurate estimation of the bias bounds since they are crucial information for good position estimation. More studies will be carried out to resolve the problem (22) and to get better estimate of the bias in the sense of maximum likelihood estimation.

## ACKNOWLEDGMENTS

The authors would like to thank the French Space Agency (CNES) for founding this research project: SPRING Usage

for Modeling Multipath Effects on a Receiver (SUMMER).

## REFERENCES

- [1] L. Wang, P. D. Groves, M. K. Ziebart, "GNSS Shadow Matching: Improving Urban Positioning Accuracy Using a 3D City Model with Optimized Visibility Prediction Scoring," *Proceedings of the 25th International Technical Meeting of The Satellite Division of the Institute of Navigation (ION GNSS 2012)*, Nashville, TN, September 2012, pp. 423-437.
- [2] P. D. Groves, Z. Jiang, L. Wang, M. K. Ziebart, "Intelligent Urban Positioning using Multi-Constellation GNSS with 3D Mapping and NLOS Signal Detection," *Proceedings of the 25th International Technical Meeting of The Satellite Division of the Institute of Navigation (ION GNSS 2012)*, Nashville, TN, September 2012, pp. 458-472.
- [3] A. J. Van Dierendonck, P. Fenton, and T. Ford, "Theory and performance of narrow correlator spacing in a GPS receiver," *J. Inst. Navig.*, vol. 39, no. 3, pp. 265-283, 1992.
- [4] M. S. Braasch, "Performance comparison of multipath mitigating receiver architectures," *Aerospace Conference, 2001, IEEE Proceedings.*, vol.3, no., pp.3/1309,3/1315 vol.3, 2001.
- [5] R. Ercek, P. De Doncker, F. Grenez, "Statistical Determination of the PR Error Due to NLOS-Multipath in Urban Canyons," *Proceedings of the 19th International Technical Meeting of the Satellite Division of The Institute of Navigation (ION GNSS 2006)*, Fort Worth, TX, September 2006, pp. 1771-1777.
- [6] I. Guvenc, C. C. Chong, "A Survey on TOA Based Wireless Localization and NLOS Mitigation Techniques," *IEEE Communications Surveys & Tutorials*, vol.11, no.3, pp.107-124, 3rd Quarter 2009.
- [7] A. H. Mohamed, "Robust and Reliable Kalman Filtering of GPS Data," *Proceedings of the 9th International Technical Meeting of the Satellite Division of The Institute of Navigation (ION GPS 1996)*, Kansas City, MO, September 1996, pp. 1441-1450.
- [8] P. Petrus "Robust Huber adaptive filter," *IEEE Trans. Signal Processing*, vol. 47, no. 4, pp.1129-1133, Apr. 1999.
- [9] K. D. Rao, M. N. S. Swamy, E. I. Plotkin, "GPS Navigation with Increased Immunity to Modeling Errors," *IEEE Transactions on Aerospace and Electronic Systems*, Vol. 40, No. 1, January 2004
- [10] K. Fellahi, C. T. Cheng, M. Fattouche, "Robust Positioning in the Presence of Outliers under Weak GPS Signal Conditions," *IEEE Systems Journal*, Vol. 6, No. 3, September 2012.
- [11] T. Perälä, "Robust Kalman-type Filtering in Positioning Applications," *Kalman Filter, Vedran Kordic (Ed.)*, ISBN: 978-953-307-094-0, InTech, DOI: 10.5772/9578. Available from: <http://www.intechopen.com/books/kalman>

- filter/robust-kalman-type-filtering-in-positioning-applications.
- [12] T. Delaporte, R. J. Landry, M. Sahnoudi, J. C. Guay, "A Robust RTK Software for High-Precision GPS Positioning," Annual European Navigation Conference, Sep. 2008.
- [13] W. Li, D. Gong, M. Liu, J. Chen, D. Duan, "Adaptive robust Kalman filter for relative navigation using global position system," *IET Radar Sonar and Navigation*, 7(5), 2013.
- [14] M. A. Gandhi, L. Mili, "Robust Kalman Filter Based on a Generalized Maximum-Likelihood-Type Estimator," *IEEE Transactions on Signal Processing*, vol.58, no.5, pp.2509-2520, May 2010.
- [15] A. Rabauoui, N. Viandier, J. Marais, E. Duflos, "Using Dirichlet Process Mixtures for the Modelling of GNSS Pseudorange Errors in Urban Canyon," *Proceedings of the 22nd International Technical Meeting of The Satellite Division of the Institute of Navigation (ION GNSS 2009)*, Savannah, GA, September 2009, pp. 2391-2399.
- [16] M. Spangenberg, J. Y. Tourneret, V. Calmettes, G. Duchateau, "Detection of variance changes and mean value jumps in measurement noise for multipath mitigation in urban navigation," *Signals, Systems and Computers, 2008 42nd Asilomar Conference on*, vol., no., pp.1193-1197, 26-29 Oct. 2008.
- [17] P. D. Groves, Z. Jiang, "Height Aiding, C/N<sub>0</sub> Weighting and Consistency Checking for GNSS NLOS and Multipath Mitigation in Urban Areas," *IEEE Communications Surveys & Tutorials*, Vol. 11, No. 3, Third Quarter 2009.
- [18] S. Peyraud, D. Betaille, S. Renault, M. Ortiz, F. Mougél, D. Meizel, F. Peyret, "About Non-Line-Of-Sight Satellite Detection and Exclusion in a 3D Map-Aided Localization Algorithm," *Sensors* **2013**, 13, 829-847.
- [19] J. Marais, S. Tay, A. Flancquart, C. Meurie, "Weighting with the pre-knowledge of GNSS signal state of reception in urban areas," European Navigation Conference, pp. 7, France, April 2015
- [20] A. Bourdeau, M. Sahnoudi, J.-Y. Tourneret, "Constructive use of GNSS NLOS-multipath: Augmenting the navigation Kalman filter with a 3D model of the environment," *15th International Conference on Information Fusion (FUSION)*, 2012, vol., pp.2271-2276, 9-12 July 2012.
- [21] A. Bourdeau, M. Sahnoudi, J.-Y. Tourneret, "Tight Integration of GNSS and a 3D City Model for Robust Positioning in Urban Canyons," *Proceedings of the 25th International Technical Meeting of The Satellite Division of the Institute of Navigation (ION GNSS 2012)*, Nashville, TN, September 2012, pp. 1263-1269.
- [22] K. A. Bin Ahmad, M. Sahnoudi, C. Macabiau, A. Bourdeau, G. Moura, "Reliable GNSS Positioning in Mixed LOS/NLOS Environments Using a 3D Model," *European Navigation Conference (ENC 2013)*, Vienne, Austria, 1-7 February 2014.
- [23] R. Kumar, M. G. Petovello, "A Novel GNSS Positioning Technique for Improved Accuracy in Urban Canyon Scenarios Using 3D City Model," *Proceedings of the 27th International Technical Meeting of The Satellite Division of the Institute of Navigation (ION GNSS+ 2014)*, Tampa, Florida, September 2014, pp. 2139-2148.
- [24] T. Suzuki, N. Kubo, "Correcting GNSS Multipath Errors Using a 3D Surface Model and Particle Filter," *Proceedings of the 26th International Technical Meeting of The Satellite Division of the Institute of Navigation (ION GNSS+ 2013)*, Nashville, TN, September 2013, pp. 1583-1595.
- [25] S. Miura, S. Hisaka, S. Kamijo, "GPS multipath detection and rectification using 3D maps," *Intelligent Transportation Systems - (ITSC), 2013 16th International IEEE Conference on*, vol., no., pp.1528-1534, 6-9 Oct. 2013
- [26] D. Betaille, F. Peyret, M. Ortiz, S. Miquel, L. Fontenay, "A New Modeling Based on Urban Trenches to Improve GNSS Positioning Quality of Service in Cities," *Intelligent Transportation Systems Magazine, IEEE*, vol.5, no.3, pp.59-70, Fall 2013
- [27] D. Betaille, F. Peyret, M. Ortiz, S. Miquel, F. Godan, "Improving Accuracy and Integrity with a Probabilistic Urban Trench Modeling," *Proceedings of the 27th International Technical Meeting of The Satellite Division of the Institute of Navigation (ION GNSS+ 2014)*, Tampa, Florida, September 2014, pp. 1891-1896.
- [28] T. Chapuis, B. Bonhoure, S. Rougerie, F. Lacoste, T. Grelier, D. Lapeyre, P. Noirat "SPRING: A Powerful 3D GNSS Simulator for Constraint Environment," *Proceedings of ION GNSS+ 2014*, Tampa, Florida, September 2014.
- [29] P. Stoica, A. Nehorai, "Performances study of conditional and unconditional direction of arrival estimation," *IEEE Trans. on SP*, 38(10): 1783-1795, 1990.
- [30] W. Kim, J. G. Lee, and G. I. Jee, "The interior-point method for an optimal treatment of bias in trilateration location," *IEEE Transaction on Vehicular Technology*, vol. 55, pp. 1291-1301, Jul. 2006
- [31] SE-NAV software from OKTAL-SE company web site <http://www.oktal-se.fr/>
- [32] "ISAE Campus", 43°34'00.29''N 1°28'32.03''E, **Google Earth**, 5/7/2013, 18/06/2015.
- [33] J. Caffery, "Wireless Location in CDMA Cellular Radio Systems," Norwell, MA: Kluwer, 2000.